ChemComm

www.rsc.org/chemcomm

COMMUNICATION

Waveguide and ultralow-threshold amplified spontaneous emission in an aligned ordered solid state based on a highly fluorescent twin-tapered bi-1,3,4-oxadiazole derivative†

Songnan Qu,[a] Yantao Li,[a] Lijun Wang,*[a] Qipeng Lu[b] and Xingyuan Liu*[a]

Strong fluorescence and amplified spontaneous emissions (ASE) both in solution and aligned ordered solid state were observed from a twin-tapered bi-1,3,4-oxadiazole derivative, which could be used in preparing functional supramolecular architectures with ultralow-threshold ASE.

It is a goal for many scientists to achieve electrically pumped organic lasers, which could open up the prospect of compact, low cost (even disposable) visible lasers suitable for applications from the point of care diagnostics to sensing.[1–4] Despite optically pumped organic lasers having been realized at various wavelengths in the whole visible region for many decades, huge obstacles are still in the way of preparing electrically pumped organic lasers. It is a main challenge to achieve high carrier injection and high current densities in the same electrically pumped organic laser device (OLD) and reduce the concomitant strong charge-induced absorption, which are required to reach a laser threshold.

Reducing the ASE threshold is one of the key targets that allows reducing the lasing threshold and further reducing the current density and optical losses from charge-induced absorption in the "gain" medium of electrically pumped devices.[5] How to reduce the ASE threshold to an ultralow value is a hot topic. The use of a binary blend in which Förster energy transfer between an absorptive donor and an emissive acceptor takes place allows reducing the optical losses in the thin-film waveguides and decreasing the ASE threshold.[6–8] For example, a lower ASE threshold of 0.11 ± 0.05 μJ cm^{-2} (220 W cm^{-2}) was observed by doping spiro-SBCz into a wide energy gap 4,4′-bis(9-carbazole)-2,2′-biphenyl (CBP) host at a doping concentration of 6 wt%.[8] However, in blends the

composition needs to be accurately controlled and phase separation can be a problem, particularly in solution-processed materials. The "gain" medium films were commonly prepared by the methods of vacuum evaporation or spin coating, which are usually isotropic or non-oriented. Physical alignment of the small molecules or conjugated polymer chains results in alignment of their transition dipoles, which in turn leads to new and interesting optical properties.[9–14] Some reports have demonstrated lower ASE thresholds of aligning organic molecular films than their non-aligning films.[15–18] Friend *et al.* reported a method of tuning the wavelength of lasing emission with a lowered threshold by aligning poly(9,9-dioctylfluorene) molecules.[18] A much lower lasing threshold (~ 20 μJ cm^{-2}, 40 kW cm^{-2}) was observed when absorption is parallel to the aligned direction in comparison with its spin coating film (~ 40 μJ cm^{-2}, 80 kW cm^{-2}).

1,3,4-Oxadiazoles derivatives have enjoyed widespread use as electron-transporting/hole blocking materials, emitting layers in electroluminescent diodes and non-linear optical materials, due to their electron-deficient nature of the heterocycle, high photoluminescence quantum yield and good thermal and chemical stabilities.[19–21] In our previous work, we reported a series of highly fluorescent liquid crystalline bi-1,3,4-oxadiazole derivatives which could be used as useful model compounds for building functional architectures.[22–24] The novelty of our present work is revealing a promising laser material based on the twin-tapered bi-1,3,4-oxadiazole derivative (BOXD-T3, as shown in Scheme 1) and a simple solution processed method in fabricating oriented ordered architectures. High fluorescence intensity and ASE of BOXD-T3 were observed both in solution and aligned ordered solid state. In particular, an ultralow-threshold ASE (about 40 W cm^{-2}) was realized in the solution processed aligned ordered film of BOXD-T3, while no ASE phenomenon was observed in its vacuum evaporated film at the excitation power below its laser damage threshold. To the best of our

[a] Key Laboratory of Excited State Processes, Changchun Institute of Optics, Fine Mechanics and Physics, Chinese Academy of Sciences, Changchun 130033, P.R. China. E-mail: wanglj@ciomp.ac.cn, xingyuanliu@hotmail.com; Tel: +86 431 8617 6341
[b] State Key Laboratory of Applied Optics, Changchun Institute of Optics, Fine Mechanics and Physics, Chinese Academy of Sciences, Changchun 130033, P.R. China
† Electronic supplementary information (ESI) available: Experimental information, photograph of the ASE from BOXD-T3 cyclohexane solution, PL and UV absorption spectra, POM images and XRD profile of solution processed microbelts or film of BOXD-T3, photograph of the measurement of the self-waveguided behavior within a larger BOXD-T3 belt. See DOI: 10.1039/c1cc10155b
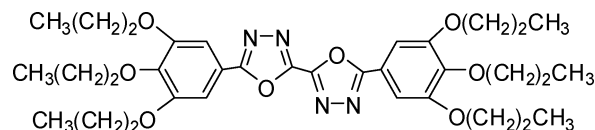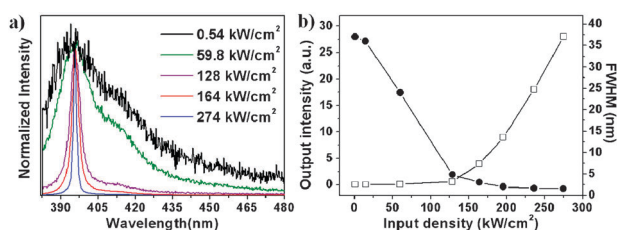

Scheme 1 Molecular structure of BOXD-T3.

Fig. 1 (a) Normalized emission spectra of BOXD-T3 in cyclohexane at 1×10^{-3} mol L^{-1} under various optically pumped pulse densities. (b) The dependence of output peak intensity ($\square$) and FWHM value ($\bullet$) of BOXD-T3 cyclohexane solution at 1×10^{-3} mol L^{-1} on pumping density.
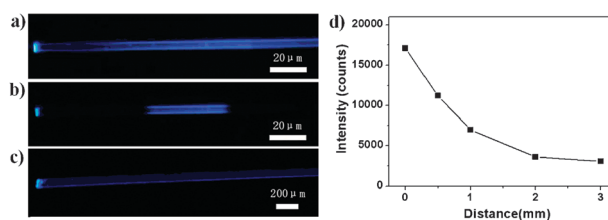

Fig. 2 Photoluminescence microscopy images of BOXD-T3 microbelts prepared in a simple slow solvent evaporation method in mixed solvents of cyclohexane/chloroform (v/v, 5 : 1). (a) The excitation UV lights were irradiated on the full observed area. (b) The excitation UV lights were refined into a ~ 50 μm spot. (c) Photoluminescence microscopy image of a large BOXD-T3 microbelt. (d) Peak intensity at maximum *versus* excitation position for the PL spectra at the tip of the large microbelt from a distance of 0–3 mm from the tip.

knowledge, it is the lowest ASE threshold under the similar pumping stripe length in a neat film ever reported.

BOXD-T3 exhibited strong fluorescence (λ_{max} = 393 nm, $\Phi_F \approx 0.96$) with a vibronic structure in dilute cyclohexane solutions. In the concentration from 1×10^{-6} mol L^{-1} to 1×10^{-3} mol L^{-1}, both shapes and maximum of the photoluminescence (PL) and UV absorption spectra remained unchanged and the fluorescent lifetime kept at about 1.4 ns, whereas the intensity of the emissions was nearly proportional to the concentrations, indicating its monomeric feature. An ultraviolet ASE (λ = 395 nm) was observed in BOXD-T3 cyclohexane solution at 1×10^{-3} mol L^{-1} with a threshold of about 125 kW cm^{-2} (Fig. 1). Increasing the excitation power above the threshold, the intensity of the ASE spectra was greatly increased, while the full width at half maximum (FWHM) of the spectra was further narrowed. At the excitation power of 274 kW cm^{-2}, the FWHM of the ASE spectrum was only 1.5 nm (Fig. S1, ESI†). The absorption spectrum of BOXD-T3 in cyclohexane showed a lack of vibronic structure, while its emission spectrum exhibited a marked vibronic structure, as seen in Fig. S2 (ESI†), which is typical of a non-planar structure in the ground state and quite a co-planar structure in the excited state,[25] indicating a four-level photophysical cycle between the ground state and excited state. Thus, it can be concluded that the co-planar structure of BOXD-T3 in the excited state and a four-level photophysical cycle between the ground state and excited state might be a reason for the strong ASE phenomenon in the monomeric state in an apolar solvent.

Straight BOXD-T3 microbelts can be prepared by a simple slow solvent evaporation method in mixed solvents of cyclohexane/chloroform or DMF/chloroform (v/v, 5 : 1). The BOXD-T3 microbelts show very strong fluorescence in the deep blue spectral region (λ_{max} = 418 nm, τ_F = 2.4 ns) with an efficiency Φ_F up to 84%. The fluorescence of the BOXD-T3 solution processed microbelts is red-shifted compared to that of its cyclohexane solution (λ_{max} = 395 nm), which may be due to the increased conjunction during BOXD-T3 molecules aggregating in an ordered solid state.[25] The PL microscopy images of the BOXD-T3 microbelts exhibit blue emission with very bright luminescence spots at tips and relatively weaker emissions from the bodies of the microbelts, which is a typical characteristic of an optical waveguide behavior (Fig. 2a). Refining the excitation UV lights into a ~ 50 μm spot, bright luminescence spots at the belt tips, which were in the unirradiated area, can also be observed (Fig. 2b). Almost all of

the observed microbelts reveal this kind of waveguide behavior. A larger BOXD-T3 belt with a width of 77 μm, thickness of 26 μm and length of about 5 mm was selected to investigate the process of light traveling along the belt (Fig. 2c). The microbelt was excited by a beam of UV light with a diameter of about 80 μm at different local positions along the length of the belt relative to a fiber-coupled charge-coupled device (CCD) spectrometer with a 400 μm pinhole that was held stationary over one of its ends (Fig. S4, ESI†). Fig. S5 (ESI†) displays the spatially resolved spectra of the self-waveguided emission that is outcoupled at the belt tip as a function of propagation length. The tip emission intensity decreases upon an increase in propagation distance. Fig. 2d shows that the peak intensity of out-coupled emissions decays exponentially with the increase in propagation distance, which is a typical characteristic of active waveguide.

Aligned microbelts or film of BOXD-T3 with a thickness of less than 1 μm could be prepared by a solvent process method, in which the glass or silicon substrates were perpendicularly immersed in the solutions. The film thickness could be controlled during the solution processing by modulating the concentrations and the solvent evaporation rates. During slow evaporation of the solvents, aligned microbelts or film grew perpendicularly to the descending solution surface (Fig. S6, ESI†). The alignment of the solution prepared film or microbelts of BOXD-T3 was demonstrated on polarized optical microscopy (POM), in which alternative changes in uniform darkness or brightness were observed by rotating the sample stage (Fig. 3a and b and Fig. S7, ESI†). The XRD profile of the BOXD-T3 aligned film consists of several sharp strong diffractions both in the low-angle range and high-angle range, indicating its crystalline feature (Fig. S8, ESI†).

Deep blue ASE (λ = 418 nm) was observed in the BOXD-T3 solution processed aligned film (thickness of about 330 nm) with an ultralow-threshold of about 40 W cm^{-2} under the focused pumping stripe (6 mm $\times$ 0.6 mm) along the alignment of the film and the polarization direction of the pumping source was perpendicular to the focused pumping stripe (Fig. 3c and d). Increasing the excitation power above the threshold, the intensity of the ASE spectra was greatly increased, while the FWHM of the spectra was further narrowed. At the excitation power of 2.3 kW cm^{-2}, the FWHM of the ASE spectrum was 5 nm. We also fabricated
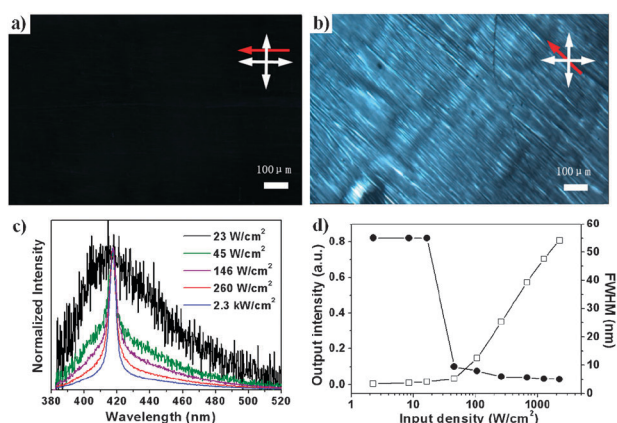
Fig. 3 (a), (b) POM images of the solution processed aligned film of BOXD-T3 on glass (white crossed arrows illustrated the crossed-polarizers and red arrow illustrated the alignment of the film). (c) Normalized photoluminescence spectra of the solution processed aligned film of BOXD-T3 on glass optically pumped at various excitation pulse densities. (d) The dependence of output peak intensity (□) and FWHM value (●) of solution processed aligned film of BOXD-T3 on glass on pumping density.

the BOXD-T3 vacuum evaporated film (about 300 nm thick) for comparison. However, no ASE phenomenon was observed in the BOXD-T3 vacuum evaporated film at the excitation power below its laser damage threshold (about 3 kW cm^{-2}).

In conclusion, strong ultraviolet ASE was observed in BOXD-T3 cyclohexane solution (1×10^{-3} mol L^{-1}) with a threshold of about 125 kW cm^{-2} and FWHM of 1.5 nm; aligned microbelts and film with strong fluorescence emissions ($\Phi_F > 80\%$) and self-waveguided structure were prepared; an ultralow-threshold ASE (about 40 W cm^{-2}) was realized in an aligned ordered film of BOXD-T3 which is the lowest ASE threshold under the similar pumping stripe length in a neat film ever reported, while no ASE phenomenon was observed in its vacuum evaporated film at the excitation power below its laser damage threshold. The co-planar structure of BOXD-T3 in the excited state and a four-level photophysical cycle between the ground state and excited state might be a reason for the strong ASE phenomenon in the monomeric state in an apolar solvent. All these results reveal that the twin-tapered bi-1,3,4-oxadiazole derivatives could be used as promising laser materials and alignment in an ordered solid state could greatly decrease the ASE threshold in this material system. This work further demonstrated that alignment of molecules in an ordered solid state can decrease the ASE threshold in

some laser materials and the method of solvent process aligned ordered film or microbelts in this work might be helpful in fabricating aligned architectures in other material systems. We expect that the highly fluorescent bi-1,3,4-oxadiazole derivatives will become a class of exciting candidates for many solid-state opto-electronic applications.

Notes and references

1. I. D. W. Samuel and G. A. Turnbull, *Chem. Rev.*, 2007, **107**, 1272.
2. I. D. W. Samuel, *Nature*, 2004, **429**, 709.
3. K. Meerholz, B. H. Wallikewitz, M. de la Rosa, J. H. W. M. Kremer and D. Hertel, *Adv. Mater.*, 2010, **22**, 531.
4. M. D. McGehee and A. J. Heeger, *Adv. Mater.*, 2000, **12**, 1655.
5. H. Yamamoto, H. Kasajima, W. Yokoyama, H. Sasabe and C. Adachi, *Appl. Phys. Lett.*, 2005, **86**, 83502.
6. S. Toffanin, R. Capelli, T.-Y. Hwu, K.-T. Wong, T. Plötzing, M. Först and M. Muccini, *J. Phys. Chem. B*, 2010, **114**, 120.
7. D. Zhang and D. Ma, *Appl. Phys. B: Lasers Opt.*, 2008, **91**, 525.
8. H. Nakanatomi, S. Akiyama, D. Ohnishi, M. Moriwake, M. Yahiro, T. Yoshihara, S. Tobita and C. Adachi, *Adv. Funct. Mater.*, 2007, **17**, 2328.
9. J. Wu, A. F. Gross and S. H. Tolbert, *J. Phys. Chem. B*, 1999, **103**, 2374.
10. Y. Che, X. Yang, K. Balakrishnan, J. Zuo and L. Zang, *Chem. Mater.*, 2009, **21**, 2930.
11. F. Gao, Q. Liao, Z. Z. Xu, Y. H. Yue, Q. Wang, H. L. Zhang and H. B. Fu, *Angew. Chem., Int. Ed.*, 2010, **49**, 6243.
12. H. Yanagi, T. Ohara and T. Morikawa, *Adv. Mater.*, 2001, **13**, 1452.
13. I. B. Martini, I. M. Craig, W. C. Molenkamp, H. Miyata, S. H. Tolbert and B. J. Schwartz, *Nat. Nanotechnol.*, 2007, **2**, 647.
14. Q. Bao, B. M. Goh, B. Yan, T. Yu, Z. Shen and K. P. Loh, *Adv. Mater.*, 2010, **22**, 3661.
15. G. Heliotis, R. Xia, K. S. Whiehead, G. A. Turnbull, I. D. W. Samuel and D. D. C. Bradley, *Synth. Met.*, 2003, **139**, 727.
16. R. Xia, M. Campoy-Quiles, G. Heliotis, P. Stavrinou, K. S. Whiehead and D. D. C. Bradley, *Synth. Met.*, 2005, **155**, 274.
17. H. Lin, C. Lin, C. Wu, T. Chao and K. Wong, *Org. Electron.*, 2007, **8**, 189.
18. M. H. Song, B. Wenger and R. H. Friend, *J. Appl. Phys.*, 2008, **104**, 033107.
19. C. Adachi, T. Tsutsui and S. Saito, *Appl. Phys. Lett.*, 1989, **55**, 1489.
20. B. Schultz, M. Bruma and L. Brehmer, *Adv. Mater.*, 1997, **9**, 601.
21. G. Hughes and M. R. Bryce, *J. Mater. Chem.*, 2005, **15**, 94.
22. S. Qu, X. Chen, X. Shao, F. Li, H. Zhang, H. Wang, P. Zhang, Z. Yu, K. Wu, Y. Wang and M. Li, *J. Mater. Chem.*, 2008, **18**, 3954.
23. S. Qu and M. Li, *Tetrahedron*, 2007, **63**, 12429.
24. S. Qu, L. Zhao, Z. Xiu and M. Li, *Langmuir*, 2009, **25**, 1713.
25. B. Valeur, *Molecular Fluorescence: Principles and Applications*, Wiley-VCH, Verlag GmbH, 2001.